Journal of Alloys and Compounds 902 (2022) 163822

Contents lists available at ScienceDirect

Journal of Alloys and Compounds

journal homepage: www.elsevier.com/locate/jalcom

Structural and magnetic alteration of Cu_2GaBO_5 forced by Mn^{3+} doping

Evgeniya Moshkina[a,*], Evgeniy Eremin[a,b,c], Dmitriy Velikanov[a], Asya Bovina[a], Maxim Molokeev[a,c,d], Yurii Seryotkin[e,f], Mikhail Cherosov[g], Ruslan Batulin[g], Ivan Nemtsev[a,c,h], Leonard Bezmaternykh[a]

[a] Kirensky Institute of Physics, 660036 Krasnoyarsk, Russia
[b] Siberian State University of Science and Technologies, 660037 Krasnoyarsk, Russia
[c] Siberian Federal University, 660041 Krasnoyarsk, Russia
[d] Department of Physics, Far Eastern State Transport University, Khabarovsk 680021, Russia
[e] Novosibirsk State University, 630090 Novosibirsk, Russia
[f] Institute of Geology and Mineralogy, 630090 Novosibirsk, Russia
[g] Institute of Physics, Kazan Federal University, 420008 Kazan, Russia
[h] Federal Research Center "Krasnoyarsk Science Center of the Siberian Branch of the Russian Academy of Sciences", 660036 Krasnoyarsk, Russia

ARTICLE INFO

Article history:
Received 12 October 2021
Received in revised form 10 January 2022
Accepted 14 January 2022
Available online 17 January 2022

Keywords:
Ludwigites
Flux growth
Magnetic susceptibility
Spin glass state

ABSTRACT

To study the gradual change of the structure and the magnetic state of the ludwigite Cu_2GaBO_5 upon Mn^{3+} doping, single crystals of $Cu_2Ga_{1-x}Mn_xBO_5$ (x = 0.55, 0.7, 0.8) with the size up to 3 × 3 × 10 mm^3 were grown using the flux technique. The phase homogeneity and crystal structure of the obtained compounds were investigated by the powder and single crystal X-ray diffraction. All the samples possessed the monoclinic-distorted ludwigite structure with the $P2_1/c$ space group. The study of the actual Cu/Ga/Mn composition by the EDX (energy-dispersive X-ray spectroscopy) technique revealed the lower Mn content in all the samples and the refined formulas were $Cu_2Ga_{0.47}Mn_{0.53}BO_5$, $Cu_{1.92}Ga_{0.5}Mn_{0.58}BO_5$ and $Cu_2Ga_{0.32}Mn_{0.68}BO_5$, respectively. Despite the high manganese content, the concentration transition (from Cu_2GaBO_5 to Cu_2MnBO_5) and change of the monoclinic angle did not occur, but strong Me-O octahedra distortions exceeding those both in the parent ludwigites Cu_2GaBO_5 and Cu_2MnBO_5 were found. The study of the thermodynamic and magnetic properties revealed the low-temperature magnetic phase transition inherited from the parent Cu_2GaBO_5 in all the samples. However, the nature and ordering type for the compounds with different Mn content were different: there was a complex transformation of the magnetic state from the partially ordered AFM (antiferromagnetically) in $Cu_2Ga_{0.47}Mn_{0.53}BO_5$, through the spin glass state, to the combined spin glass/ordered state in $Cu_2Ga_{0.32}Mn_{0.68}BO_5$ with the appearance of magnetic anisotropy. The evident dependence of T_c (phase transition temperature) on the magnetic field was found as well as its decrease at the nonzero magnetic field in the samples with x = 0.53 and 0.68.

1. Introduction

Ludwigites $M1^{3+}M2_2^{2+}BO_5$ possess a complex quasi-low-dimensional structure: the unit cell contains four nonequivalent cationic positions (Z = 4) occupied by heterovalent cations (or by cations of different types in the case of heterometallic ludwigites),which entails the formation of the complex magnetic structure and gives rise to the question about the occupation of different positions by different cations [1–6].

Copper-based ludwigites can appropriately be distinguished as a separate subgroup among other members of this family. The structure of all copper ludwigites possesses monoclinic distortions which arise due to the Jahn-Teller effect of Cu^{2+}. There are several copper ludwigites with the substitution in the trivalent subsystem: $Cu_2M^{3+}BO_5$ (M = Al, Cr, Fe, Ga, Mn) [4,7–18]. Recently, the solid solutions $Cu_2Mn_{1-x}Fe_xBO_5$ (x = 0.2, 0.4, 0.5) with the heterometallic trivalent subsystem have been obtained and studied [17], where the analysis of the field and thermal dependences of magnetization shows the high dependence of the magnetic properties on x with a change in the type of magnetic ordering and presence of the spin glass state in all the compounds.

Here, we present a new study of $Cu_2Ga_{1-x}Mn_xBO_5$ solid solutions. The magnetic properties and origin of the phase transitions of the

* Corresponding author.
E-mail address: ekoles@iph.krasn.ru (E. Moshkina).

https://doi.org/10.1016/j.jallcom.2022.163822
0925-8388/

parent compounds, Cu_2GaBO_5 and Cu_2MnBO_5, are significantly different. Cu_2GaBO_5 is an antiferromagnet with the Neel temperature T_N = 4.1 K [10,15,16]. Cu_2MnBO_5 is a ferrimagnet with T_C = 92 K [8,9]. The magnetic structure of these ludwigites were studied experimentally. Both of them demonstrate an unusual configuration of the magnetic moments. Cu_2GaBO_5 has a complex non-collinear magnetic structure with a large magnetic unit cell and destruction of the long-range magnetic order in the external magnetic field above 1 T due to the influence of the structure-disordered subsystem occupied by gallium and copper on the ordered one [16]. According to [10], two of the four nonequivalent positions are completely occupied by copper, while the other two (2*d* and $4e^2$ [8]) contain both copper and gallium Ga^{3+} with the occupation numbers 0.6 and 0.7, respectively (structure-disordered subsystem). Cu_2MnBO_5 [8] has a non-collinear ferrimagnetic structure: there are two magnetic subsystems inside which the ions are ordered antiferromagnetically. The magnetic moments of the subsystems are canted, oriented at an angle of 60º relative to each other, and the direction of the moments does not coincide with the main crystallographic directions of the crystal. The trivalent ions are located in one of these subsystems, in the position $4e^2$. It is shown that three out of four nonequivalent positions ($4e^1$, 2*d* and 2*a*) are occupied by copper cations, and the fourth position is occupied by manganese. In addition, the structure of these ludwigites is different. Despite the same space group ($P2_1/c$), there are other types of octahedra distortions in Cu_2MnBO_5 (which can be caused by the Jahn-Teller effect of Mn^{3+}): the monoclinic angle β is about 92º while for other Cu-containing ludwigites (including Cu_2GaBO_5) it is about 97º.

The study of $Cu_2Ga_{1-x}Mn_xBO_5$ solid solutions using the gradual $Ga^{3+} \rightarrow Mn^{3+}$ substitution will make it possible to observe the effects of the crystallographic and magnetic restructuring of Cu_2GaBO_5-Cu_2MnBO_5. Our hypothesis is as follows: due to the substitution of non-magnetic Ga^{3+} by Mn^{3+}in the structure-disordered subsystem of Cu_2GaBO_5, the magnetic order in the structure-disordered subsystem will change. By the sequential substitution it is possible to trace the regularity of changes in the magnetic properties in order to understand whether cationic and magnetic ordering is realized, and also to try to find out in which subsystem this occurs.

2. Experimental section

2.1. Crystal growth

$Cu_2Ga_{1-x}Mn_xBO_5$ single crystal samples were obtained using the flux method. The flux system can be written as:

$$(100-n)\%\ mass.\ (Bi_2Mo_3O_{12} + qNa_2B_4O_7) + n\%\ mass.\ \left(2CuO + \frac{1-x}{2}Ga_2O_3 + \frac{x}{2}Mn_2O_3 + \frac{1}{2}B_2O_3\right) \quad (1)$$

The mass coefficients (q and x) of the oxides in (1) and the concentration of the crystal-forming oxides are presented in Table 1.

$Bi_2Mo_3O_{12}$ – based fluxes are characterized by low viscosity and low melting temperature, and they are successfully used for crystal growth of many compounds [14]. This solvent type is used for growing many ludwigites, including Cu-containing ones [9,14], and it gives relatively low saturation temperatures, low time-dependence due to the low viscosity, and absence of the composition impurity due to the substitution by the solvent components.

Table 1
The parameters of the flux system (1): n is the concentration of the crystal forming oxides, x is the manganese content, q is the mass coefficient of $Na_2B_4O_7$.

Compound	x	q	n, %	T_{sat}, K
$Cu_2Ga_{0.2}Mn_{0.8}BO_5$	0.80	0.7	31.7	888
$Cu_2Ga_{0.3}Mn_{0.7}BO_5$	0.70	0.7	34.8	905
$Cu_2Ga_{0.45}Mn_{0.55}BO_5$	0.55	0.7	40.2	940

The fluxes in (1) were prepared by the sequential melting of the initial oxides in a platinum crucible (V = 100 cm^3) at temperature T = 1100 °C. The melting order was the following: firstly, borax ($Na_2B_4O_7$) was melted, then the Bi_2O_3 – MoO_3 – B_2O_3 powder mixture was added and Mn_2O_3 and Ga_2O_3 were added in portions, and finally, the CuO oxide was added in portions. The formation of $Bi_2Mo_3O_{12}$ upon melting the mixture of oxides Bi_2O_3 and MoO_3 is suggested in the stoichiometric ratio 1:3 [19]. After the preparation, the fluxes were homogenized during 3 h at T = 1100 °C. At the next stage, the parameters and saturation temperatures of the fluxes were determined through the observation of the crystal formation on the crystal-holder in the form of a platinum rod, which was inserted into the flux upon the sequential lowering of the temperature with the step of 5 °C to 20 °C. For each flux, the high-temperature crystallizing phase in quite a wide temperature range (not smaller than 40 °C) was the ludwigite phase. The crystals were in the form of elongated prisms.

Single crystals of $Cu_2Ga_{1-x}Mn_xBO_5$ solid solutions were grown at spontaneous nucleation. After homogenization the temperature in the furnace was reduced rapidly from T = 1100 °C down to (T_{sat} − 5) °C at a rate of 100 °C/h. Then, the temperature lowering rate was dT/dt = 2 °C/day. After 4 days the crystal holder was removed from the flux, and the grown crystals in the form of black elongated prisms with the size up to 3 × 3 × 10 mm^3 were separated from the crystal-holder and the flux remainder was removed by etching in 20% aqueous solution of nitric acid.

2.2. XRD (X-ray diffraction)

The X-ray patterns of the $Cu_2Ga_{1-x}Mn_xBO_5$ (x = 0.55, 0.7, 0.8) powders were obtained using a D8 ADVANCE powder diffractometer (Cu-radiation, Vantec linear detector, the apertures −0.6 mm, the step size of 2θ – 0.016°, the counting time – 0.5 s, the angle range – 5–70°) and the X-ray data on the powders were obtained using the analytical equipment of the Krasnoyarsk Center for Collective Use, SB RAS. For the identification of the studied compounds, the program Search-Match was used.

The single crystal diffraction data were collected under ambient conditions on an Oxford Diffraction Xcalibur Gemini diffractometer (MoKα radiation, 0.5 mm collimator, graphite monochromator) equipped with a CCD-detector. The data reduction, including the background correction and Lorentz and polarization corrections, was performed using the *CrysAlisPro* 171.38.43 software [20]. The semi-empirical absorption correction was applied by the multi-scan technique. The structures were solved by the direct methods and refined within the anisotropic approach using the SHELX-97 program package [21]. The supplementary crystallographic data were deposited in the Inorganic Crystal Structure Database (CSD 2111370) and can be obtained from the Cambridge Crystallographic Data via https://www.ccdc.cam.ac.uk/structures/.

2.3. EDX (energy-dispersive X-ray spectroscopy)

The morphological aspects of the samples as well as the chemical composition were characterized with a TM4000 Plus (Hitachi, Japan) in the BSE (backscattered electrons) mode using an acceleration voltage of 20 kV and equipped with an EDX XFlash Detector 630Hc (Bruker, Germany). The sample preparation was performed as follows. $Cu_2Ga_{1-x}Mn_xBO_5$ (x = 0.55, 0.7, 0.8) was mounted with a carbon conductive double coated SEM (scanning electron microscopy) adhesive (Ted Pella, Inc., USA) on a SEM sample aluminum stub (Hitachi, Japan). It should be noted that no conductive films were coated on the sample surface prior to making the SEM measurements. Nevertheless, the electrical conductivity of the crystals was

Table 2
The space group and lattice parameters of the $Cu_2Ga_{1-x}Mn_xBO_5$ oxyborates obtained by the powder X-ray diffraction. The data for Cu_2GaBO_5 are taken from [15] and given for comparison.

Compound	*a*, Å	*b*, Å	*c*, Å	*β*, deg	*V*, Å^3	Space group
$Cu_2Ga_{0.2}Mn_{0.8}BO_5$	3.15814(3)	11.9957(1)	9.4113(1)	96.4909(6)	354.255(7)	$P2_1/c$
$Cu_2Ga_{0.3}Mn_{0.7}BO_5$	3.14350(3)	11.9835(2)	9.4435(2)	97.2382(9)	352.905(9)	$P2_1/c$
$Cu_2Ga_{0.45}Mn_{0.55}BO_5$	3.13116(4)	11.9661(1)	9.4681(2)	97.7221(8)	351.532(8)	$P2_1/c$
Cu_2GaBO_5[15]	3.1121	11.9238	9.4708	97.865	348.137	$P2_1/c$

sufficient to avoid charging of the surface. To investigate the chemical composition of the specimens and uniformity of the element distribution over the surface, the X-ray elemental mapping technique was employed within a 12,288 μm^2 square. The acquisition time was the same for all the samples and amounted to 5 min.

2.4. Magnetic measurements

The temperature-field dependences of magnetization and temperature dependences of *ac*-susceptibility of the synthesized samples were obtained in the temperature range of 4.2–300 K and in the magnetic fields up to 9T using the PPMS-9 (Quantum Design) and SQUID-magnetometers developed in the Kirensky Institute of Physics SB RAS [22,23].

2.5. Specific heat measurements

The specific heat was measured by the relaxation method using PPMS-9 (Quantum Design) in the temperature range 1.8 K < *T* < 300 K and in the magnetic fields up to 9 T.

3. Crystal structure

The crystal structure of the obtained $Cu_2Ga_{1-x}Mn_xBO_5$ ($x = 0.55$, 0.7, 0.8) was studied by the powder X-ray diffraction. The phase homogeneity of the obtained samples was confirmed. The space group and the lattice parameters are presented in Table 2. All the samples belong to the $P2_1/c$ space group and they are isostructural to the Cu_2GaBO_5 parent compound. Table 2 includes the corresponding parameters for Cu_2GaBO_5 for comparison [15].

The substitution of $Ga^{3+}$with the Jahn-Teller Mn^{3+} cation leads to the structural changes accompanied by the changes in the lattice parameters (Table 2). The dependences of the lattice parameters on the cation concentration in the flux are presented in Fig. S1. The unit cell volume dependence is close to the linear law. With the manganese content increasing, the unit cell volume also increases, which is in agreement with the difference of the Ga^{3+} and Mn^{3+} ionic radii ($R(Ga^{3+}) = 0.620$ Å, $R(Mn^{3+}) = 0.645$ Å). The lattice parameters *a* and *b* also increase with the increase in the manganese content, in correspondence with the larger Mn^{3+} ionic radii. However, on the contrary, *c* and *β* monoclinic angles decrease. This is caused by the difference of the different monoclinic distortion types of Cu_2GaBO_5 and Cu_2MnBO_5 due to the non-isostructurality of these compounds. The transition between these structures has to be accompanied by the change of monoclinic axis due to the presence of the Jahn-Teller Mn^{3+} cation and symmetry of other Mn-O octahedra [9]. To study the structural distortions in the Cu-Mn-Ga ludwigites, the X-ray diffraction experiment was performed using the single crystal sample.

To study the actual content of the grown ludwigites $Cu_2Ga_{1-x}Mn_xBO_5$, the element-selective technique EDX was applied. The homogeneity and high quality of all the samples were confirmed by the results of X-ray mapping and SEM (scanning electron microscopy) (Fig. S2). The obtained percentages of Cu, Mn and Ga in the crystals are presented in Table 3. The accuracy of the EDX study of the content is quite high (about 5%) for the main elements (Mo and heavier elements). In the case of Cu, Ga and Mn, the measurement error can be higher. As one can see in Table 3, the EDX composition of the crystals is different from that in the flux. This can be explained by the difference of the partition coefficients of gallium and manganese oxides: the solubility of Mn_2O_3 exceeds the solubility of Ga_2O_3 in the fluxes used (1). Thus, the actual gallium content exceeds the one in the flux for all the samples. The least difference has been revealed for the sample with $x = 0.55$ in the flux: for this compound the actual manganese concentration is $x = 0.53$, that almost match the determined one. The maximum manganese content in the obtained crystals is 0.68 instead of 0.8 and it is still quite high. Though the Cu_2GaBO_5/Cu_2MnBO_5 phase boundary was not reached, the compound $Cu_2Ga_{0.2}Mn_{0.8}BO_5$ ($Cu_2Ga_{0.32}Mn_{0.68}BO_5$) is the nearest one. A further increase in the manganese content should be studied, which is planned for the future. Further the EDX concentrations will be used.

A sample of $Cu_{1.92}Ga_{0.5}Mn_{0.58}BO_5$ was selected for the single crystal X-ray diffraction experiment. The main crystal data are shown in Table 4. The occupation of mixed cation positions was refined taking into account their full populations. The atomic coordinates, occupancy, and displacement parameters for the refined structure are presented in Table 5 and S1. The selected distances and angles are listed in Table 6. The studied sample crystallizes in a monoclinically distorted structure of the ludwigite mineral (Fig. 1). The unit cell metrics is monoclinic, and the space group is $P2_1/c$. The studied compound is isostructural to Cu_2MnBO_5 [9] and Cu_2GaBO_5 [15]. The cations are statistically distributed over four nonequivalent positions. M1 and M4 are in general positions, M2 and M3 are in a special one with the symmetry –1. In the general positions, the cations of all the three types are located; the special positions are statistically occupied by Cu and Mn. It should be noted that the parent Cu_2GaBO_5 has another cation distribution over the nonequivalent positions: M1 and M2 are occupied by Cu, while M3 and M4 are the mixed positions occupied by Cu and Ga [15,16]. This means that the presence of manganese and gallium in the structure can cause another cation distribution over four nonequivalent positions. The refined formula unit of the compound under study can be presented as $Cu_{1.887(10)}Ga_{0.313(6)}Mn_{0.802(13)}BO_5$. In comparison with the initial ratio of the cations in the flux the refined formula has

Table 3
The results of the EDX experiments: the percentages of Cu, Mn and Ga and the EDX composition of $Cu_2Ga_{1-x}Mn_xBO_5$.

Element/Composition in the flux	$Cu_2Ga_{0.2}Mn_{0.8}BO_5$	$Cu_2Ga_{0.3}Mn_{0.7}BO_5$	$Cu_2Ga_{0.45}Mn_{0.55}BO_5$
Cu	66	64	66
Mn	23	19	18
Ga	11	17	16
EDX composition	$Cu_2Ga_{0.32}Mn_{0.68}BO_5$	$Cu_{1.92}Ga_{0.5}Mn_{0.58}BO_5$	$Cu_2Ga_{0.47}Mn_{0.53}BO_5$

Table 4
The crystal structure parameters of $Cu_{1.92}Ga_{0.5}Mn_{0.58}BO_5$.

Space group, *Z*	$P2_1/c$, 4
a (Å)	3.14190(6)
b (Å)	11.9844(2)
c (Å)	9.43628(17)
β (deg.)	97.1684(18)
V (Å^3)	352.533(11)
Reflections measured / independent / with $I > 2\sigma(I)$ / R_{int}	10,963 / 1784 / 1619 / 0.0659
h, *k*, *l*- limits	$-5 \le h \le 5$; $-20 \le k \le 20$; $-15 \le l \le 15$
R1 / *wR2* / *Goof* for the observed reflections $[I > 2\sigma(I)]$	0.0339 / 0.0804 / 1.089
R1 / *wR2* / *Goof* for all the data	0.0381 / 0.0842 / 1.087
$\Delta\rho_{max}$ / $\Delta\rho_{min}$ (e/Å^3)	2.642 / −1.965

some excess of Mn and a lack of Cu, while the amount of Ga is in good agreement. Unfortunately, ESD (estimated standard deviations) is large; therefore, the obtained composition can be different from the actual one due to the X-ray scattering factors of manganese and copper atoms (but manganese and gallium can be distinguished much better) being similar. This was the case for Cu_2MnBO_5, as was shown earlier [9].

R1, wR2 and GooF are the indicators of the structure refinement quality: $R1 = \sum(|F_{obs}| - |F_{calc}|)/\sum|F_{obs}|$, $wR2 = \left\{\sum\left(w\left(F_{obs}^2 - F_{calc}^2\right)^2\right)/\sum\left(w\left(F_{obs}^2\right)^2\right)\right\}^{1/2}$,, where w,F_{obs}, F_{calc} are the weight, observed and calculated structure factors of reflection, respectively, n and p are the reflection number and the number of the parameters to be refined, respectively.

The coordinating environment of the analysis of the cation positions (Table 5) shows the preservation of the octahedral coordination typical for orthorhombic ludwigites [24] only for the special M3 position. It should be noted that similar cation octahedral environment distortions were observed in the structures of the parent Cu_2MnBO_5 and Cu_2GaBO_5 [9,15]. However, the octahedra symmetry of the studied $Cu_{1.92}Ga_{0.5}Mn_{0.58}BO_5$ can be analyzed in comparison with the symmetry of the parent compounds (see Supporting information).

The analysis shows the preservation of the Cu_2GaBO_5-type octahedra distortions only for the M2 position. Apparently, this position with a high probability is occupied by the Cu^{2+} ions and is not affected by the trivalent subsystem substitution. Strong changes appear in the M4 position environment: its symmetry type transforms to the M4 position in Cu_2MnBO_5. But, it is not necessary for Mn^{3+} in the Cu_2GaBO_5 structure to occupy only the position M4 ($4e^2$) as in Cu_2MnBO_5. The octahedra of the remaining positions (M1 and M3) change the distortion type relative to both parent compounds which allows the mixed filling of these positions.

Despite the fact that the structure of $Cu_{1.92}Ga_{0.5}Mn_{0.58}BO_5$ inherits the regularities of both parent compounds, the lattice parameters are closer to the copper-gallium ludwigite taking into account the large manganese content in comparison with the gallium one. This may indicate that the change in the $Cu_2GaBO_5 \rightarrow Cu_2MnBO_5$ structure (ex.: change in the β angle) can have a threshold character when the monoclinic distortions resulting in the structure characterized by Jahn-Teller Mn^{3+} exceed the critical value (this hypothesis is confirmed by the extreme values of the Me-O long distances of the M1 and M4 octahedra).

Table 6
The selected distances (Å) for $Cu_{1.92}Ga_{0.5}Mn_{0.58}BO_5$.

M1–O4	1.917 (2)	M3–O5 (2 ×)	1.9818 (17)
M1–O2	1.9243(19)	M3–O4(2 ×)	2.043(3)
M1–O3	1.9944(18)	M3–O4(2 ×)	2.134(2)
M1–O1	2.0128(17)		
M1–O2	2.106(2)	M4–O2	1.9045(18)
M1–O4	2.637(3)	M4–O4	1.949(2)
		M4–O3	2.0106(18)
M2–O2(2 ×)	1.9610(17)	M4–O5	2.0260(18)
M2–O1(2 ×)	1.9886(17)	M4–O5	2.4022(19)
M2–O1(2 ×)	2.4381(19)	M4–O3	2.449(2)
B1–O1	1.371(3)		
B1–O5	1.375(3)		
B1–O3	1.377(3)		

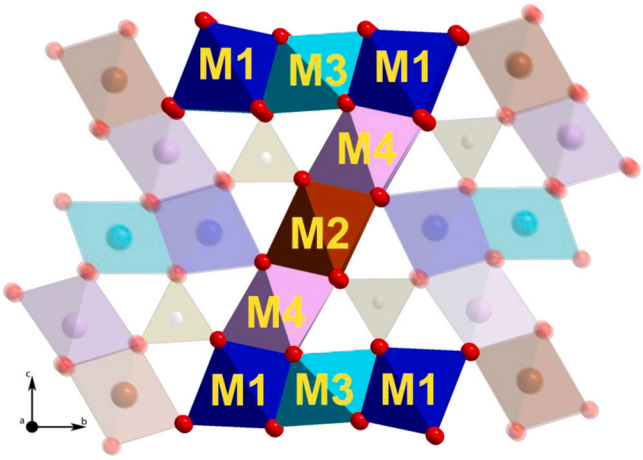

Fig. 1. The ludwigite structure. The main structural element in the shape of *Z* is highlighted. It is composed of the Me-O octahedra. M1, M2, M3, M4 are the nonequivalent cation positions occupied with different probability by the cations Cu^{2+}, Mn^{3+} and Ga^{3+}.

4. Magnetic properties

The thermal dependences of magnetization of the synthesized samples $Cu_2Ga_{1-x}Mn_xBO_5$ ($x = 0.53, 0.58, 0.68$) were obtained at $H||a$ and $H\perp a$ (H = 1 kOe) in the FC and ZFC modes and they are presented in Fig. 2. As light kink of the FC curve is observed on the magnetization dependence of each sample in the low temperature range. This anomaly corresponds to the magnetic phase transition. As the

Table 5
The atomic parameters for $Cu_{1.92}Ga_{0.5}Mn_{0.58}BO_5$.

Site	Occupancy	*x*	*y*	*z*	U_{eq}
M1	$Cu_{0.493(3)}Ga_{0.219(3)}Mn_{0.288(4)}$	0.45477(10)	0.38072(2)	0.77098(3)	0.01072(9)
M2	$Cu_{0.780(4)}Mn_{0.219(5)}$	0	0.5	0	0.00854(11)
M3	$Cu_{0.728(4)}Mn_{0.272(5)}$	0.5	0.5	0.5	0.00798(11)
M4	$Cu_{0.640(3)}Ga_{0.094(3)}Mn_{0.268(4)}$	−0.01123(9)	0.28032(3)	0.50703(3)	0.01053(9)
B1	1.00	0.4787(9)	0.3645(2)	0.2345(3)	0.0101(4)
O1	1.00	0.5418(6)	0.53829(14)	0.84264(19)	0.0125(3)
O2	1.00	−0.0334(6)	0.35553(14)	0.9017(2)	0.0138(3)
O3	1.00	0.4488(6)	0.23671(14)	0.6648(2)	0.0146(3)
O4	1.00	0.0597(9)	0.42229(17)	0.6080(2)	0.0286(5)
O5	1.00	0.5260(6)	0.36434(14)	0.3813(2)	0.0127(3)

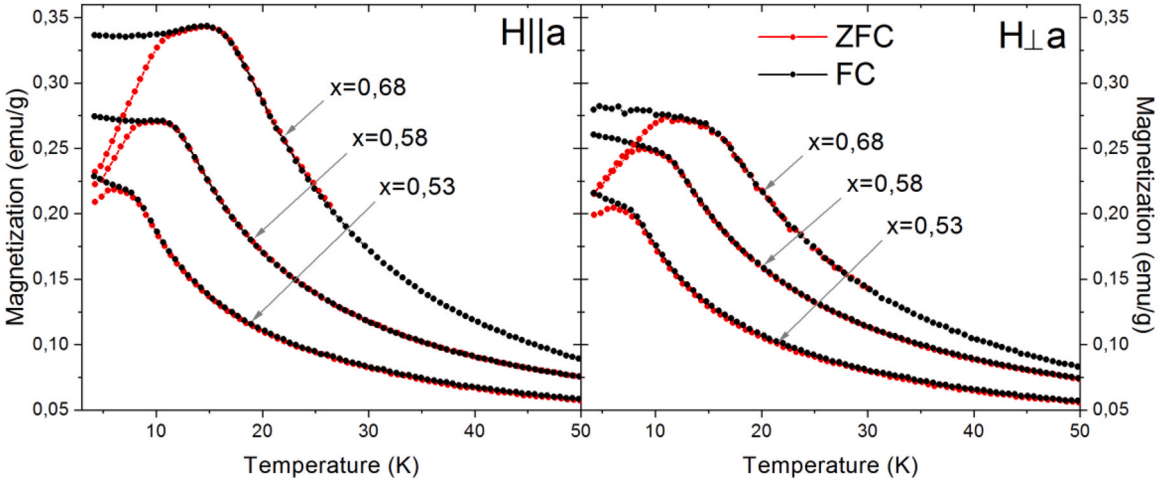

Fig. 2. The thermal dependences of magnetization of $Cu_2Ga_{1-x}Mn_xBO_5$ ($x = 0.53, 0.58, 0.68$) obtained at $H = 1$ kOe with the $H||a$ and $H\perp a$ magnetic field orientations in the FC (black) and ZFC (red) modes using PPMS.

manganese content increases, the phase transition temperature and magnetization increase as well. In Cu_2GaBO_5, ions of Cu^{2+} form planes with the possible interaction way through the M4 [15,16]. The occupation of M4 by the nonmagnetic cation (Ga^{3+}) makes these planes isolated from each other. So the system is characterized by quasi-one-dimensional or quasi-two-dimensional magnetic ordering with the corresponding low T_C. The increasing of T_C at addition of Mn^{3+} can be caused by the origin of three-dimensional magnetic structure (ex. Cu_2MnBO_5 [8,9]). The obtained dependences are in a qualitative agreement with those for the Cu_2GaBO_5 parent compound where this phase transition corresponds to antiferromagnetic ordering [15].

An interesting feature of the obtained curves is the thermal dependence of magnetization in the ordered phase (Fig. 2). Below the transition temperature, the curves obtained at $H||a$ and $H\perp a$ behave differently in each sample. The magnetization in the $H||$a direction demonstrates a weak growth for the sample with $x = 0.53$, or an almost constant law is observed for $x = 0.68$ and $x = 0.58$ samples: the slope of the curve changes smoothly with the increasing manganese content. The analogous dependence obtained at $H\perp a$ increases with the decreasing temperature for all the samples (however, here the tendency towards the slope reduction can also be observed). In the Cu_2GaBO_5 parent ludwigite all the dependences increase at the same rate. This increase in paramagnetic magnetization indicates the incomplete ordering of the magnetic moments upon the mentioned phase transition [16]. The calculation of the exchange interactions of the Cu_2GaBO_5 ludwigite shows that in the system there is a competition of the exchange interactions, and some exchange interactions are close to zero, which can lead to not fully ordered weakly related subsystems [16,25]. The experimental investigation of the magnetic structure of Cu_2GaBO_5 shows the existence of the long-range ordering in the crystal formed by the M1 and M2 positions. However, the M3 and M4 positions remain disordered, which explains the increase in the paramagnetic magnetization below T_C. The addition of manganese (Mn^{3+} is located in the M4 position in Cu_2MnBO_5 following NPD (neutron powder diffraction) [8]) can lead to the "completion" of the magnetic structure of the copper-gallium ludwigite and, to a great extent, to the influence on the long-range magnetic order in the crystal. The addition of manganese causes the appearance of new competing interactions and reduces the number of the magnetic moments, which do not participate in the magnetic phase transition. Indeed, the slope of the magnetization dependences of the synthesized samples increases from sample to sample with the increasing manganese content in the low temperature phase.

Several analogous measurements of the temperature dependences of magnetization were carried out using PPMS and SQUID-magnetometers. The comparison of the obtained curves shows the qualitative conformity: the conditional correspondence of the phase transition temperatures and the behavior of the curves in the low-temperature phases for each sample. However, there are important differences: different "widths" of the susceptibility peaks in the vicinity of the phase transition, different slopes of the curves in the paramagnetic phase approaching the transition temperature (Fig. 3).

The temperature dependence of magnetization of the studied solid solutions corresponds to the analogous curves obtained for pure Cu_2GaBO_5 [15]. As compared with Cu_2GaBO_5, with the increasing manganese concentration, the total magnetic moment and phase transition temperature predictably increase. Despite this, based on the performed study, the authors suppose the type of magnetic ordering in the samples with $x = 0.58$ and 0.68 to be significantly different from the parent antiferromagnetic compound. The magnetic moments in the low temperature phase of these compounds, can be partially disordered and the spin glass state is observed. The consideration and comparison of the results obtained using equipment with different magnetization measurement techniques reveal in detail the divergence of the curves in the low-temperature range in the vicinity of the phase transition. This

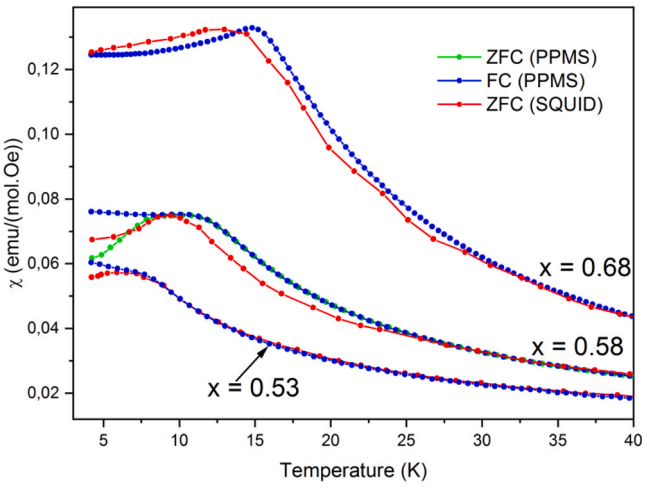

Fig. 3. The $\chi(T)$ curves obtained using the PPMS and SQUID magnetometers. The concentrations x are given in agreement with EDX results (Table 3).

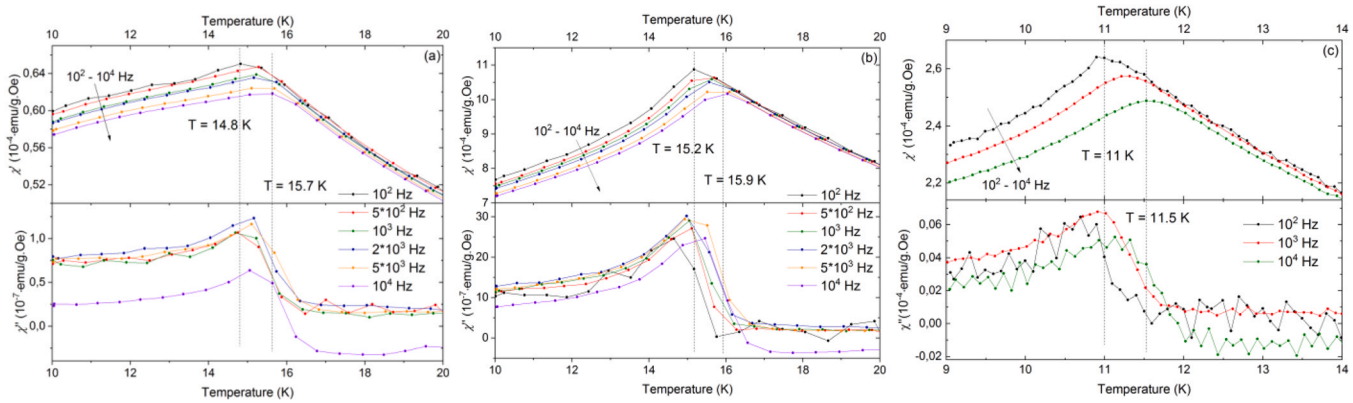

Fig. 4. The thermal dependences of *ac*-susceptibility of $Cu_2Ga_{0.32}Mn_{0.68}BO_5$ (a – $H \perp a$, b – $H||a$) and $Cu_{1.92}Ga_{0.5}Mn_{0.58}BO_5$ (c – powder sample).

reflects the presence of time-dependent factors, such as long relaxation time characterizing the processes of the magnetic moment reorientation relative to the direction of the applied magnetic field.

One can suppose the magnetic sample state to be closer to saturation during the PPMS magnetization measurements for each temperature point. This could explain a larger magnetic moment measured by PPMS than the one measured using SQUID-magnetometer for the same temperatures. The influence of the relaxation processes on the magnetization measurements in the paramagnetic phase can be explained by the presence of the short-range correlation arising above T_C. This is supported by the nonlinear dependence of the inverse magnetic susceptibility (discussed below) in a wide temperature range.

Such differences of the temperature curves are observed for the samples with $x = 0.58$ and 0.68. The sample with the lower manganese content ($x = 0.53$) does not demonstrate this behavior: the temperature magnetization dependence does not depend on the measurement method in the whole temperature range. This can indicate the absence of the spin glass state in $Cu_2Ga_{0.47}Mn_{0.53}BO_5$. The low temperature phase of this compound is most likely to be antiferromagnetic as is the case for the parent Cu_2GaBO_5.

The thermal dependences of the real and imaginary part of *ac*-susceptibility of the samples with $x = 0.68$ and $x = 0.58$ is presented in Fig. 4. The real part demonstrates a peak corresponding to the magnetic phase transition detected using *dc*-magnetization measurements. The peak position depends on the frequency of the applied magnetic field and shifts with T_C increasing in the range of $T = 14.8$ K to $T = 15.7$ K for the sample with $x = 0.68$ and in the range of $T = 11$ K to $T = 11.5$ K for the sample with $x = 0.58$ with an increase in the corresponding frequency (from 10^2 Hz to 10^4 Hz). The thermal dependence of the imaginary part demonstrates a kink in the vicinity of the phase transition. Such behavior of *ac*-susceptibility indicates the presence of the spin glass phase in $Cu_2Ga_{0.32}Mn_{0.68}BO_5$ and $Cu_{1.92}Ga_{0.5}Mn_{0.58}BO_5$. To check the existence of a spin glass behavior the frequency dependence of the peak in $\chi'(T)$ has been analyzed using Mydosh parameter calculation [26–28]:

$$\Omega = \frac{T_2 - T_1}{T_2 \cdot (\log \nu_2 - \log \nu_1)}; \quad (2)$$

The calculated parameters are $\Omega = 0.0287$ for the sample with $x = 0.68$ ($H \perp a$), $\Omega = 0.022$ for the sample with $x = 0.68$ ($H||a$) and $\Omega = 0.0217$ for the sample with $x = 0.58$ (powder sample). The typical Mydosh parameter for canonical spin glass systems is known to vary from 0.004 to 0.02 [27]. The spin glasses with the higher value can be characterized as cluster SG systems [26].

The magnetic structure changes with the increase in the manganese content in $Cu_2Ga_{1-x}Mn_xBO_5$ are also manifested in field dependences of magnetization (Fig. 5). For comparison, Fig. 5 also

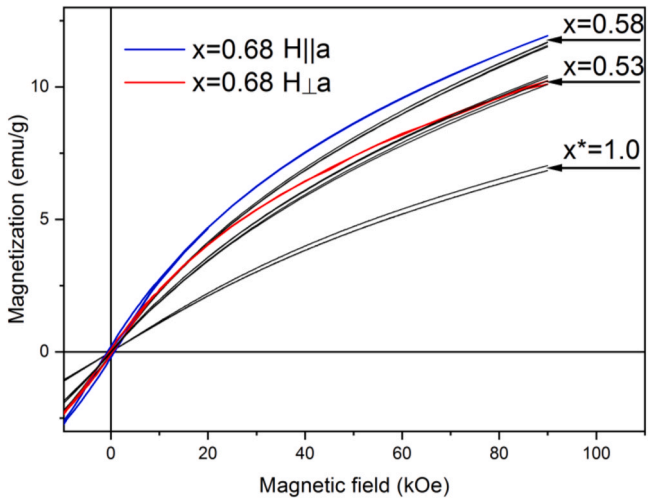

Fig. 5. The magnetic field dependences of magnetization of the single crystals $Cu_2Ga_{1-x}Mn_xBO_5$ ($x = 0.53$, 0.58, 0.68) obtained at $T = 4.2$ K in both magnetic field orientations $H||a$ and $H \perp a$. To compare, the magnetic field dependences of magnetization of the Cu_2GaBO_5 single crystal obtained at $T = 2$ K in the magnetic field orientations $H||a$ and $H \perp a$ are added.

presents the field dependences of magnetization of the single crystal Cu_2GaBO_5 obtained at $T = 2$ K in the magnetic field orientations $H||a$ and $H \perp a$. These dependences are identical to the ones obtained earlier [15]. One can see that the analogous curves obtained for the samples with $x = 0.53$ and $x = 0.58$ qualitatively match the curves obtained for the sample without substitution: the changes are manifested only in the increase of the total magnetic moment with the increasing manganese content. The total magnetic moment of all the samples including Cu_2GaBO_5 obtained at $H||a$ is slightly larger than the one obtained at $H \perp a$. As one can see in Fig. 5, the magnetic anisotropy of the samples with $x = 0.53$ and $x = 0.58$ is almost zero. In the sample with $x = 0.68$ the field dependences obtained at $H||a$ and $H \perp a$ demonstrate other behavior: there appears the anisotropy of magnetic properties and even without any significant increase in the total magnetic moment as related to the sample with the lower manganese content.

The increased anisotropy of magnetic properties in $Cu_2Ga_{0.32}Mn_{0.68}BO_5$ can be analyzed along with the conclusion on the presence of the spin glass state in the following way. The ludwigite structure is relatively complex and contains four nonequivalent positions of magnetic cations. Due to the symmetry, the splitting of the magnetic structure to the subsystems formed by two couples of cation positions is typical for ludwigites. For pure Cu_2GaBO_5 these are the M1-M2 antiferromagnetic subsystem and

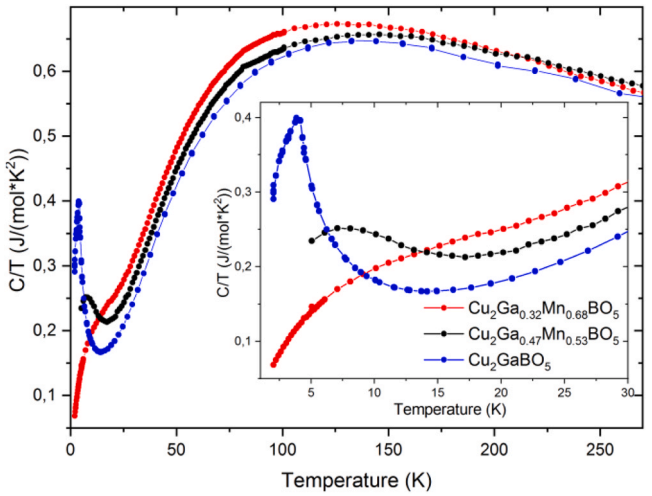

Fig. 6. The thermal dependences of the specific heat $C/T\,(T)$ of $Cu_2Ga_{1-x}Mn_xBO_5$ ($x = 0$, 0.53, 0.68) measured in the zero magnetic field.

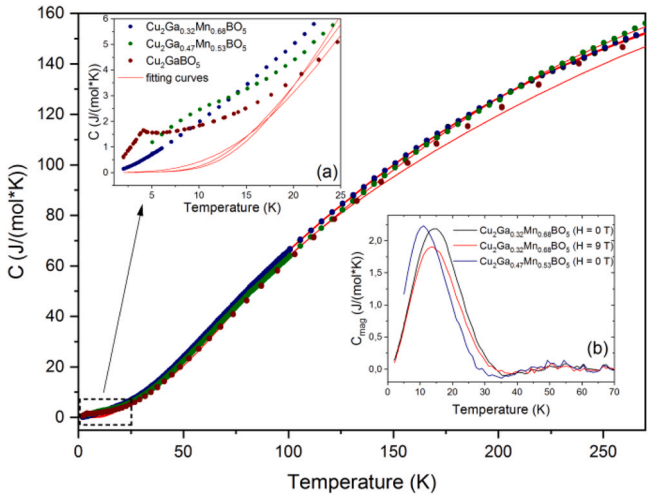

Fig. 7. The thermal dependences of the specific heat $C(T)$ of $Cu_2Ga_{1-x}Mn_xBO_5$ ($x = 0$, 0.53, 0.68) measured in the zero magnetic field presented along with the fitting of the experimental curves (denoted by the red lines). Inset (a): low temperature range up to 25 K; it shows the transformation of the $C(T)$ curves with the increasing manganese content and the comparison of the experimental curves and the fitting. Inset (b): magnetic contribution to the specific heat obtained as the difference between the experimental data and the lattice contribution (fitting); the data presented for $Cu_2Ga_{0.47}Mn_{0.53}BO_5$ (blue line) and $Cu_2Ga_{0.32}Mn_{0.68}BO_5$ (black line) at the zero magnetic field and for $Cu_2Ga_{0.32}Mn_{0.68}BO_5$ (red line) obtained at $H = 9$ T.

M3-M4 disordered couple. In $Cu_2Ga_{0.32}Mn_{0.68}BO_5$ the coexistence of the antiferromagnetic phase as in the parent Cu_2GaBO_5 and spin glass phase caused by particular filling of M4 by Mn^{3+} is possible.

The obtained field dependences of the synthesized $Cu_2Ga_{1-x}Mn_xBO_5$ ($x = 0.58$, 0.68) have hysteresis loops. The coercive field of the sample with $x = 0.58$ is the same for both directions of the applied magnetic field ($H||a$ and $H\perp a$) and equal to $H_c \approx 0.4$ kOe ($T = 4.2$ K). In the case of the sample with $x = 0.68$, which demonstrates the anisotropy of the field dependences, the coercive field values are also different for two magnetic field directions ($H||a$ and $H\perp a$) and these are $H_c^{\perp} \approx 0.4$ kOe and $H_c^{//} \approx 0.7$ kOe ($T = 4.2$ K), respectively. The loop shape does not depend on the orientation of the sample and it does not differ from sample to sample.

5. Specific heat measurements

Specific heat measurements of the samples with $x = 0.68$ ($H = 0$ T, 9 T) and $x = 0.53$ ($H = 0$ T) were performed. Figs. 6 and 7 show the obtained specific heat $C/T(T)$ and $C(T)$ dependences of the studied samples in comparison with the pure Cu_2GaBO_5. In the low temperature range (up to 30 K) small anomalies corresponding to the magnetic phase transitions were found in both samples. These anomalies are much less pronounced than for Cu_2GaBO_5 and blurred with the increasing manganese concentration (inset (a) in Fig. 7). The $C/T(T)$ dependences presented in Fig. 6 show these anomalies more clearly: the lambda-like specific heat peak of Cu_2GaBO_5 becomes much smoother as the manganese content increases with the transition temperature growth. T_C (the phase transition temperature) of the samples with $x = 0.53$, 0.68 cannot be accurately determined at this stage due to smoothing. In Fig. 6 one can clearly see the increase in the specific heat value for every graph point with the addition of manganese, which is in agreement with the increase in the manganese content in the flux from sample to sample.

The comparison of the specific heat dependences obtained in the zero and nonzero ($H = 9$ T) magnetic field for the sample with $x = 0.68$ shows a decrease in T_C and even stronger anomaly smoothing. The same behavior was observed in Cu_2GaBO_5 [16], suggesting the destruction of the long-range AFM order by the small magnetic field (of the order of 2.5 T).

6. Discussion

The anomaly of the thermal dependence of the specific heat of Cu_2GaBO_5 discussed in [15] is a λ-shaped peak, which indicates the AFM ordering being established in the sample. The Mn-doped compounds show quite smooth specific heat peaks, which can indicate the destruction of the long range order or, as mentioned above, the spin glass state of a part of magnetic positions in comparison with the parent Cu_2GaBO_5. The peak shape is highly dependent on the manganese content as it becomes smoother with the manganese content increase. The specific heat anomaly of the compound with 0.8 of manganese is just slightly visible in the $C(T)$ dependence and can be distinguished in the $C/T(T)$ dependence. The observed type of the specific heat anomaly in many cases describes systems with the spin glass state [29].

To specify the magnetic contribution to the specific heat, the fitting of the experimental curves was made according to [15,30]:

$$C = C_{latt} + C_{mag} \quad (3.1)$$

$$C_{latt} = \alpha_D \cdot C_D + \alpha_{E1} \cdot C_{E1} + \alpha_{E2} \cdot C_{E2} + \alpha_{E3} \cdot C_{E3} \quad (3.2)$$

The specific heat can be considered as a sum of two parts (3.1): the lattice specific heat C_{latt} and the magnetic specific heat C_{mag}. To specify the magnetic contribution to the specific heat it is necessary to determine the lattice contribution and extract it from the total C according to (3.1): $C_{mag} = C - C_{latt}$. The lattice specific heat can be obtained by fitting the experimental curve using (3.2) in the temperature range above the phase transition. A minimized set of fit parameters was employed using a sum of one isotropic Debye term (C_D) accounting for 3 acoustic phonon branches and three isotropic Einstein terms (C_{E1}, C_{E2}, C_{E3}) averaging the optical phonon branches, $3s - 3 = 24$ [15]. The ratio between these terms was fixed to $\alpha_D{:}\alpha_{E1}{:}\alpha_{E2}{:}\alpha_{E3} = 1{:}2{:}2{:}4$ to account for the $3s = 27$ degrees of freedom per formula unit ($s = 9$ atoms per formula unit).

The resulting fit curves (Fig. 7) are in good agreement with the experimental data above 50 K. The obtained Einstein and Debye temperatures (3.2) are presented in Table 7. In [15] the fitting was performed using two Einstein terms. The reduction of the Einstein terms to 2 does not provide a good agreement of the fit curves and experimental data in the present study. Thus, the obtained results on the Einstein temperatures can hardly be compared with the earlier obtained data for the parent Cu_2GaBO_5 [15]. The Debye temperature agrees well with the one for Cu_2GaBO_5. The calculated magnetic

Table 7
The obtained fitting parameters of the $C(T)$ curve fitting: Debye (θ_D) and Einstein temperatures (θ_{E1}, θ_{E2}, θ_{E3}).

Compound	H, T	θ_D, K	θ_{E1}, K	θ_{E2}, K	θ_{E3}, K
$Cu_2Ga_{0.47}Mn_{0.53}BO_5$	0	169.97	266.16	441.08	865.61
$Cu_2Ga_{0.32}Mn_{0.68}BO_5$	0	155.15	267.11	409.35	889.59
	9	153.92	269.11	405.79	899.12

contribution to the specific heat (3.1) is presented in the inset (b) of Fig. 7. The dependences $C_{mag}(T)$ have the anomalies in the form of quite wide peaks in the low temperature range, indicating the magnetic phase transition in the compounds with 0.53 and 0.68 of manganese. The phase transition temperature for the sample with $x = 0.68$ is in good agreement with the value obtained from the magnetization and *ac*-susceptibility measurements. But T_C of the sample with $x = 0.53$ exceeds the critical temperature obtained by the measurements of the magnetic properties, being equal to 11 K (instead of 8–9 K). This difference can be caused by the effects of the magnetic ordering suppression by the external magnetic field inherited from the parent Cu_2GaBO_5. Therefore, one can conclude that the magnetic ordering type of $Cu_2Ga_{0.47}Mn_{0.53}BO_5$ is similar to the pure copper-gallium ludwigite.

Based on the obtained specific heat dependences and calculated entropy of the phase transitions (which is about 2.5–3 J/(mol·K) for the studied samples instead of the theoretically needed 25.6 and 29 J/(mol K) for full ordering [8]) it is suggested that in the studied samples all or a part of the cation positions should not be magnetically ordered and the spin glass state be realized. It is necessary to note that the phase transition entropy of Cu_2GaBO_5 approximately is equal to those obtained for the Mn-substituted samples. This could mean the same ordering level in these samples.

To determine the phase transition temperatures (T_c) two approaches were used based on the plots $\partial M^2/\partial T(T)$ or $\partial(\chi T)/\partial T(T)$, which is followed by the comparison of the results and estimation of their applicability. According to the molecular field theory, the magnetic contribution to the specific heat is proportional to the squared spontaneous magnetization (usually used for ferromagnets) [31]. The thermal dependences of the temperature derivative of the squared magnetization are presented (Fig. 8). The $\partial M^2/\partial T(T)$ dependences were built for both magnetic field orientations $H||a$ and $H\perp a$. As one can see in Fig. 8, all the dependences in the low temperature range demonstrate the maximum, indicating the magnetic phase transition. It is seen that the temperatures T_C of the samples with $x = 0.58$ and $x = 0.68$ are different at different external magnetic field orientations. Here, the difference for the sample with $x = 0.58$ is about $\Delta T_C \approx 0.6$ K, for the sample with $x = 0.68$ this difference increases and it is about $\Delta T_C \approx 1.8$ K. The directional dependence of the phase transition temperature confirms the appearance and growth of the anisotropy of the magnetic properties as a consequence of the gallium → manganese substitution.

In [32] it is shown that in a simple antiferromagnet with predominantly short-range interactions, the magnetic specific heat C_m is proportional to $\partial(\chi T)/\partial T$. Plotting $\partial(\chi T)/\partial T$ vs. T (Fig. 9) shows the lowering of the phase transition temperature for each sample relative the results of both specific heat (at $H = 0$) and *ac*-susceptibility measurement results. The data obtained from the $\partial(M^2)/\partial T$ vs. T plot have a similar slope, but the value of T_c for the compound with the higher manganese content significantly exceeds both other values (Fig. 10). Analyzing the comparison of the data given in Fig. 10 one can conclude that the use of the $\partial(\chi T)/\partial T$ vs. T (for antiferromagnets [32–34]) or $\partial(M^2)/\partial T$ vs. T (usually, for ferromagnets [31]) plots to determine T_c is poorly valid for the studied systems due to the magnetic phase mixture: antiferromagnetic and spin glass phases. But it is shown that the phase transition temperature of the studied ludwigites is highly dependent on the value of the applied magnetic

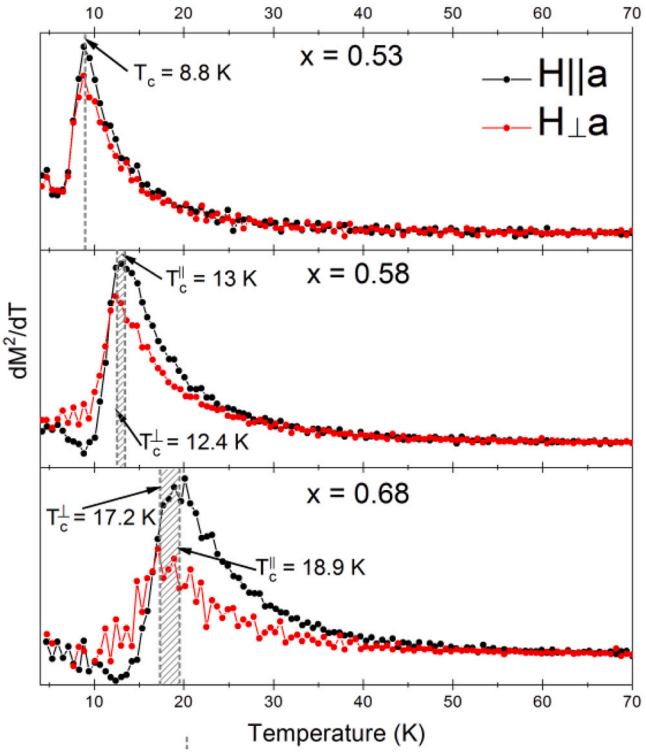

Fig. 8. The thermal dependences of the temperature derivative of the squared magnetization of $Cu_2Ga_{1-x}Mn_xBO_5$ ($x = 0.53$, 0.58, 0.68) obtained using the magnetization measurements at the magnetic field orientations $H||a$ and $H\perp a$.

field. Despite the inconsistency of the obtained data the phase transition temperature T_c hysteresis is observed both in $\partial(M^2)/\partial T$ vs. T (Fig. 8) and *ac*-susceptibility vs. T (Fig. 4) (the comparison has made for the sample with $x = 0.68$).

T_c of the samples $Cu_2Ga_{0.32}Mn_{0.68}BO_5$ (11 K), $Cu_{1.92}Ga_{0.5}Mn_{0.58}BO_5$ (11.5 K) and $Cu_2Ga_{0.47}Mn_{0.53}BO_5$ (14.5 K) determined by the direct techniques (open circles in Fig. 10) along with the data for the parent Cu_2GaBO_5 (4.1 K [15]) show an almost linear dependence on the Mn content. Small deviation of T_c for $Cu_{1.92}Ga_{0.5}Mn_{0.58}BO_5$ can indicate the influence of lower Cu^{2+} content (as it was determined by EDX).

Despite the fact that the determination of the phase transition temperature of the current ludwigites via the $\partial(\chi T)/\partial T$ vs. T plot is doubtful, quite ambiguous results were obtained: two peaks in the $\partial(\chi T)/\partial T(T)$ plot for $Cu_2Ga_{0.32}Mn_{0.68}BO_5$ and $Cu_{1.92}Ga_{0.5}Mn_{0.58}BO_5$ were found, which can indicate two magnetic phase transitions. The clear evidence for this was found in $Cu_{1.92}Ga_{0.5}Mn_{0.58}BO_5$ for both magnetic field directions ($H||a$, $H\perp a$). In $Cu_2Ga_{0.47}Mn_{0.53}BO_5$ these two peaks are not so pronounced due to the low Tc (few experimental points in the low temperature range), but the effect can also be seen for both magnetic field directions. The specific heat anomaly of $Cu_2Ga_{0.47}Mn_{0.53}BO_5$ is quite blurred and, with some probability, can contain two peaks.

The approximation of the thermal dependences of inverse magnetic susceptibility of the obtained $Cu_2Ga_{1-x}Mn_xBO_5$ ($x = 0.53$, 0.58, 0.68) was performed in the paramagnetic phase using the modified Curie-Weiss law [35]:

$$\chi = \chi_0 + \frac{C}{T - \theta} \quad (4)$$

As the experimental dependences deviate from the linear law, the temperature-independent contribution χ_0 was singled out as a separate term. It consists of the diamagnetic contribution and Van

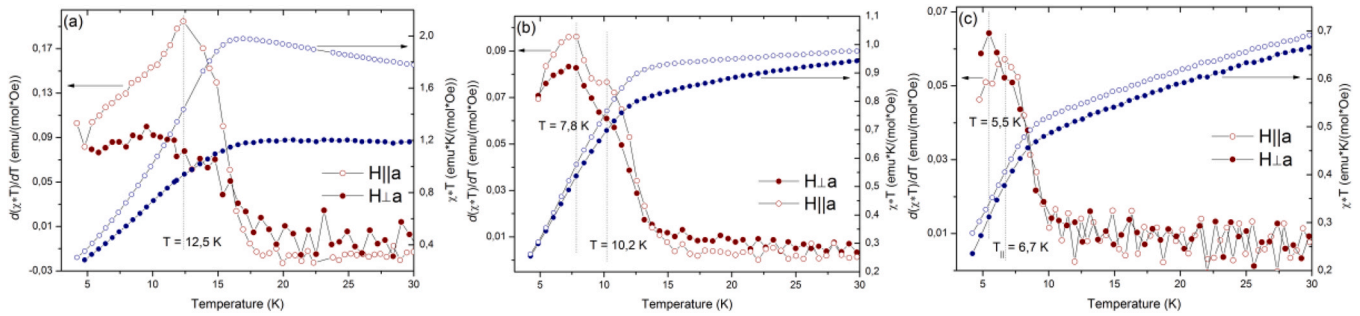

Fig. 9. Plot of the computed $\partial(\chi T)/\partial T(T)$ (wine color) and $\chi T(T)$ (navy color) obtained from the ZFC data of the magnetic susceptibility for $Cu_2Ga_{0.32}Mn_{0.68}BO_5$ (a), $Cu_2Ga_{0.42}Mn_{0.58}BO_5$ (b), $Cu_2Ga_{0.47}Mn_{0.53}BO_5$ (c) for both $H||a$ and $H\perp a$.

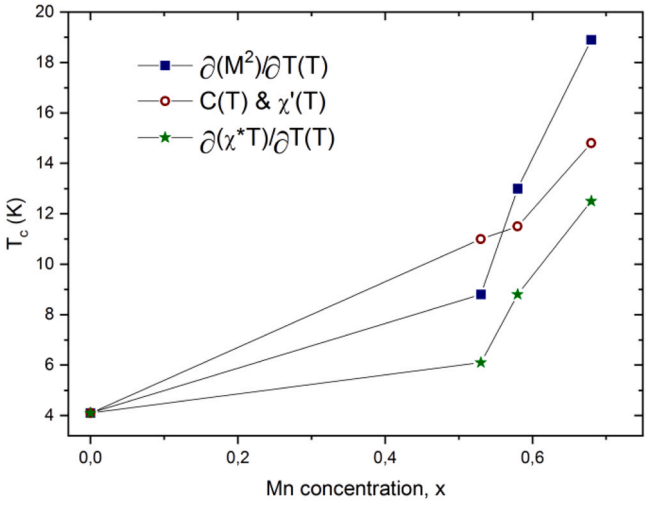

Fig. 10. Comparison of the phase transition temperature (T_c) dependences on the Mn content obtained via the $\partial(\chi T)/\partial T(T)$ plot ($H||a$, green stars), $\partial(M^2)/\partial T(T)$ plot (navy squares) and specific heat (at $H = 0$) and *ac*-susceptibility measurements (wine circles).

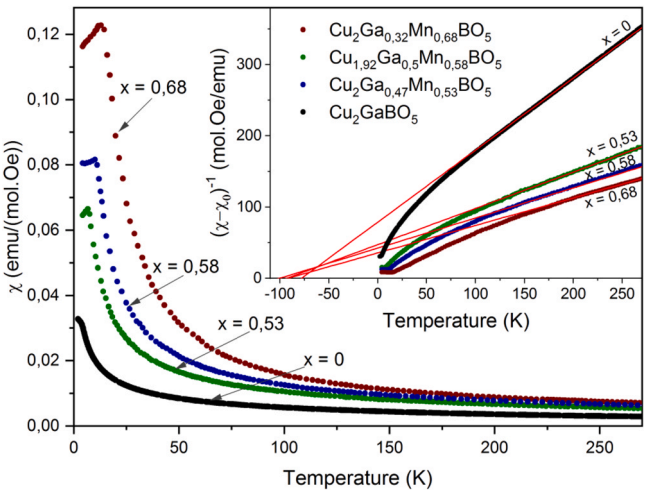

Fig. 11. The temperature dependence of the molar magnetic susceptibility of $Cu_2Ga_{1-x}Mn_xBO_5$ ($x = 0.53$, 0.8, 0.68) and Cu_2GaBO_5, $H||a$. The temperature dependence of the inverse magnetic susceptibility and its fitting (red lines) is given in the inset.

Vleck paramagnetism: $\chi_0 = \chi_d + \chi_{VV}$; C is the Curie constant; θ is the paramagnetic Curie-Weiss temperature.

Following the modified Curie-Weiss law (4), the temperature-independent contribution χ_0 can be obtained as a limit $\chi \to \chi_0$ at $T \to \infty$. For this purpose, plotting χ vs $1/T$ and determining χ_0 in the limit of $1/T = 0$ can be done using the linear extrapolation with the focus on the high temperature data points [26]. The magnetization measurements of the sample with $x = 0.58$ with the following estimation of the molar magnetic susceptibility were made up to 792 K (Fig. S3), and an attempt to estimate χ_0 via the χ vs $1/T$ dependence was made. However, the experimental curve $\chi(1/T)$ does not behave linearly in the area of the high temperatures even up to 792 K. Thus, these measurements are not able to give the actual χ_0 value.

Due to the presence of three fitting parameters (too many) the approximation did not give reliable results at the initial stage. Therefore, it was necessary to reduce the quantity of the fitting parameters: the temperature-independent term was estimated theoretically and the fitting was done using two parameters, namely, the Curie constant C and paramagnetic temperature θ.

The diamagnetic susceptibility was calculated by summing the Pascal constants $\chi_d = \sum_i \chi_{di}$ for each atom in the formula unit (it is tabulated in [36]). The paramagnetic Van Vleck contribution of the Mn^{3+} cations for each obtained compound was calculated using the expression $\chi_{VV} = 8\,N{\cdot}\mu_B{}^2/\Delta$ derived in [37–39], where Δ is the energy gap between the ground-state ($t2g$) and excited (eg) levels. To estimate χ_{VV} the energy gap of Mn^{3+} cations was taken as $\Delta = 1.8$ eV [36]. The Van Vleck contribution of Cu^{2+} cations is much lower than for Mn^{3+}, and thus, it was not taken into account [39]. The manganese concentration and the corresponding molar mass were taken in agreement with the Cu/Ga/Mn content obtained by EDX (see Table 3). The temperature-independent terms are presented in Table 8.

The temperature dependence of molar magnetic susceptibility, taking into account χ_0, and the fitting are presented in Fig. 11, including the data for Cu_2GaBO_5. In the low temperature range, at about 60–100 K above the phase transition temperature, the dependences start deviating from the linear law. This can be accounted for by the short-range correlations appearing in the paramagnetic

Table 8
The molar masses and estimated temperature-independent contribution to magnetic susceptibility of $Cu_2Ga_{1-x}Mn_xBO_5$ ($x = 0.53$, 0.58, 0.68): diamagnetic susceptibility (χ_d), paramagnetic Van Vleck susceptibility (χ_{VV}) and its sum (χ_0).

Compound	M (g/mol)	$\chi_d{\cdot}10^{-4}$ (emu/(mol Oe))	$\chi_{VV}{\cdot}10^{-4}$ (emu/(mol Oe))	$\chi_0{\cdot}10^{-4}$ (emu/(mol Oe))
$Cu_2Ga_{0.32}Mn_{0.68}BO_5$	277.600	-0.904	0.317	-0.587
$Cu_{1.92}Ga_{0.5}Mn_{0.58}BO_5$	279.542	-0.899	0.272	-0.627
$Cu_2Ga_{0.47}Mn_{0.53}BO_5$	279.788	-0.901	0.251	-0.650

Table 9
The Curie-Weiss temperatures and effective magnetic moments obtained from the experimental $(\chi - \chi_0)^{-1}(T)$ curves and calculated using (3). The experimental parameters were calculated by fitting the $(\chi - \chi_0)^{-1}(T)$ curves obtained at $H||a$ and $H\perp a$. The data for Cu_2GaBO_5 were taken from [15].

Compound	θ, K $H\|\|a$	θ, K $H\perp a$	C, $\frac{emu \cdot K}{mol \cdot Oe}$ $H\|\|a$	μ_{eff}^{exp}, μ_B $H\|\|a$	C, $\frac{emu \cdot K}{mol \cdot Oe}$ $H\perp a$	μ_{eff}^{exp}, μ_B $H\perp a$	μ_{eff}^{theor}, μ_B	x_{calc}
$Cu_2Ga_{0.32}Mn_{0.68}BO_5$	-88.69	-83.75	2.58	4.54	2.62	4.58	4.86	0.57
$Cu_{1.92}Ga_{0.5}Mn_{0.58}BO_5$	-101.74	-86.36	2.39	4.38	2.25	4.24	4.57	0.46
$Cu_2Ga_{0.47}Mn_{0.53}BO_5$	-93.09	-87.13	1.97	3.97	1.86	3.85	4.47	0.34
Cu_2GaBO_5	-69	-74		2.79		2.73	2.63	–

phase. With the increase in the manganese concentration the linear law range shifts to the high temperature region. The fitting was done in the 170–270 K temperature range for all the samples (inset in Fig. 11). The results of the approximation, Curie-Weiss temperatures θ, Curie constants C were determined from the fitting of $1/(\chi\text{-}\chi_0)$ vs. T for each sample, at both directions of the magnetic field ($H||a$, $H\perp a$), and these are presented in Table 9. The experimental effective magnetic moments were calculated using the relation $\mu_{eff}^2 = 3k_B C/N_A$ for $H||a$ and $H\perp a$ (Table 9). The values of the experimentally obtained effective magnetic moments agree with the increase in the manganese content in the samples. The difference of μ_{eff}^{exp}, obtained at $H||a$ and $H\perp a$, is lower than 3%. The difference between the θ temperatures in different solid solutions is about 1–3 K ($H\perp a$) and 5–13 K ($H||a$); as compared to Cu_2GaBO_5 this difference is about 13–20 K for each magnetic field direction. This qualitatively agrees with the small x step in the solid solutions and with the significant difference in the manganese concentration in comparison with Cu_2GaBO_5.

The calculation of the theoretically expected values of the effective magnetic moments of all $Cu_2Ga_{1-x}Mn_xBO_5$ ($x = 0.53$, 0.58, 0.68) was performed using the formula:

$$\mu_{eff}^2 = \mu_B^2 \cdot \sum_i N_i \cdot \mu_i^2 \quad (5.1)$$

$$\mu_i^2 = g_i^2 \cdot S \cdot (S+1) \quad (5.2)$$

where i is the type of magnetic ion (Cu^{2+} or Mn^{3+}), N_i is the number of i type ions in the formula unit, g_i is the Lande g-factor of the ions with i type (g (Cu^{2+}) = 2.2 [15], g (Mn^{3+}) = 2 [30]), S is the spin moment of the i^{th} ion (S (Cu^{2+}) = 1/2, S (Mn^{3+}) = 2), μ_B is the Bohr magneton. The g-factor value of the Cu^{2+} ion corresponds to the experimentally obtained one for Cu_2GaBO_5 [15]. The calculated effective moments are also presented in Table 8. One can see that the theoretically expected moments exceed the experimentally obtained ones. On average, the difference for each solid solution is almost constant (0.6 μ_B). Here, the experimental and theoretical effective moments for Cu_2GaBO_5 are in good agreement between each other. The obtained difference between the experimental and theoretical moments of the $Cu_2Ga_{1-x}Mn_xBO_5$ ($x = 0.53$, 0.58, 0.68) indicates the possible inconsistency of the taken Cu/Ga/Mn ratio with the actual composition. The manganese content x_{calc} that corresponds to the experimental effective magnetic moments was calculated using (5) $(\mu_{eff}^{exp})^2 = \mu_B^2 \cdot 2g_{Cu2+}^2 \cdot S_{Cu2+}(S_{Cu2+}+1) + \mu_B^2 \cdot x_{calc} \cdot g_{Cu2+}^2 \cdot S_{Cu2+} \cdot (S_{Cu2+}+1)$, and the data are presented in Table 9. The results are significantly different from the ratio in the flux (on average, 0.2) and these are 0.57, 0.46, 0.34 (averaged values) versus $x = 0.68$, 0.58, 0.53 obtained by EDX, respectively.

A possible way of the deviation origin can be revealed taking into account the dependence of the effective magnetic moment on the g-value of Cu^{2+} (the g-value of Mn cations is not considered due to the small value of possible deviations from 2 [40,41]) and cation concentration. The g-value for Cu^{2+} (g = 2.2) is taken from [15] (the g-value is taken as the average between 2.00 and 2.40 - the minimum and maximum values measured for Cu^{2+} [42]), and thus, the results of the calculation are comparable with the data of Cu_2GaBO_5 where this g value is in very good agreement with the experiment. In addition, changing the g-value for Cu^{2+} even up to the extreme values is not enough to explain the effective magnetic moment deviation due to the small Cu^{2+} spin value: the calculated effective magnetic moment of the sample with $x = 0.68$ for $g = 2$ and $g = 2.4$ and the results are μ_{eff} ($g = 2$) = 4.72 μ_B and μ_{eff} ($g = 2.4$) = 5.00 μ_B, which still exceeds, to some extent, the experimental values 4.54 μ_B and 4.58 μ_B. Thus, the reduction of the theoretical μ_{eff} can be due to the manganese content decrease, indicating the inconsistence of the content used and the actual one.

The values of the effective magnetic moments μ_{eff}^{exp} have been obtained from the fitting of the experimental curves $(\chi - \chi_0)^{-1}(T)$. The values of μ_{eff}^{exp} can match the theoretical ones μ_{eff}^{theor} in the case of its increasing, i.e. increasing of Curie constants C. The fitting was done using minimal set of parameters (C and θ) including theoretical estimation of χ_0. The fitting of $\chi(T)$ over three parameters C, θ and χ_0 gave much less C (in comparison with Table 9) and quite high positive χ_0 indicating the huge Van Vleck contribution that doesn't agree with the other works and with the experimental attempts to determine χ_0 from high-temperature (up to 792 K) magnetization measurements done in the present work.

Thus, discarding the exotic cases of the low spin state of manganese cations (Mn^{3+} or Mn^{2+}), the only reason for the theoretical and experimental effective magnetic moment deviation is the difference of the taken and the actual composition. The authors suppose that this problem deserves an additional attention and will be studied using wide range of methods in the nearest future.

7. Conclusions

The study presents the investigation results of the growth, structure, thermodynamic and magnetic properties of new solid solutions $Cu_2Ga_{1-x}Mn_xBO_5$ ($x = 0.53$, 0.58, 0.68) with the ludwigite structure. These compounds “build a bridge” between the parent antiferromagnetic Cu_2GaBO_5 and ferrimagnetic Cu_2MnBO_5, which, despite the isostructurality, demonstrate a significant difference not only in the magnetic properties but also in the structural ones. The solid solutions were obtained using the flux method; the developed flux system with the optimized parameters allowed growing crystals of the sufficient size to provide orientational measurements of the magnetic properties. The structure was studied using several techniques and the results showed the distortions inherited from both parent compounds in the considered crystals. When dealing with the flux method, the investigation of the actual crystal composition is of high importance. The lower contribution of manganese than that of gallium was shown for all the samples, meaning the difference of the partition coefficients of Mn_2O_3 and Ga_2O_3 in the fluxes used. This result will help to correct the flux composition in the future in order to achieve the desired ratio of Mn/Ga not only in the studied system.

Based on the results of this study, one can conclude that the phase boundary Cu_2GaBO_5/Cu_2MnBO_5 is still not reached: the structural and magnetic properties of all three compounds $Cu_2Ga_{1-x}Mn_xBO_5$ ($x = 0.53$, 0.58, 0.68) are closer to Cu_2GaBO_5 despite the high manganese concentration. However, the changes in the magnetic properties are well pronounced and the following statements can be formulated:

- The paramagnetic growth of magnetization in the low temperature phase stops with the increasing manganese content. This means that manganese enters one or both paramagnetic positions M3 and M4 of Cu_2GaBO_5, making all the positions contribute to the magnetic phase transition.
- The magnetic ordering type of $Cu_2Ga_{0.47}Mn_{0.53}BO_5$ is similar to pure copper-gallium ludwigite. A significant shift of the magnetic phase transition temperature recorded with and without the external magnetic field was found. The applied magnetic field of 1 kOe reduces T_C from 11 K to 8 K (down to 6.7 K in agreement with $\partial(\chi T)/\partial T$ vs. T plotting), which corresponds to the destruction of the AFM long range order by the magnetic field similar to Cu_2GaBO_5.
- The magnetic restructuring in the Cu_2GaBO_5 – Cu_2MnBO_5 row occurs through the phase containing the spin glass state. Based on the specific heat, *dc*-magnetization and *ac*-susceptibility measurements, the presence of the spin glass state in the manganese doped samples with $x = 0.58$ and 0.68 was revealed. However, it is possible that the magnetic moments of not all four cation positions freeze in both samples. The phase transition entropy of the sample with $x = 0.68$ is almost equal to the corresponding one of antiferromagnetic Cu_2GaBO_5. Thus, the ordering in the copper subsystem can persist, which concerns the M1-M2/M3-M4 subsystem interactions, which are much weaker than intra-subsystem interactions [25].
- The appearance of the magnetic anisotropy detected in the field dependences of magnetization in $Cu_2Ga_{0.32}Mn_{0.68}BO_5$ distinguishes this sample from other obtained Cu-Ga-Mn ludwigites (including the parent Cu_2GaBO_5). Despite obvious evidence of the presence of the spin glass state in this sample, this indicates the changes in the magnetic structure and, possibly, partial restoration of the magnetic ordering.

The study of crystallographic and magnetic restructuring of the ludwigites $Cu_2Ga_{1-x}Mn_xBO_5$ ($x = 0.53$, 0.58, 0.68) at the current stage shows a number of interesting effects giving rise to an idea of microscopic processes occurring due to doping with Mn. To build the whole phase diagram for Cu_2GaBO_5 – Cu_2MnBO_5 and present it in detail and to describe this concentration transition it is necessary to obtain and study samples with a higher manganese content which is planned in the nearest future.

CRediT authorship contribution statement

Evgeniya Moshkina: Conceptualization, Methodology, Investigation, Validation, Visualization, Writing – review & editing. **Evgeniy Eremin:** Resources, Data curation. **Dmitriy Velikanov:** Resources, Data curation. **Asya Bovina:** Data curation. **Maxim Molokeev:** Software, Resources, Data curation, Writing – review & editing. **Yurii Seryotkin:** Software, Resources, Data curation. **Mikhail Cherosov:** Resources, Data curation. **Ruslan Batulin:** Resources, Data curation. **Ivan Nemtsev:** Resources, Data curation. **Leonard Bezmaternykh:** Conceptualization, Supervision.

Declaration of Competing Interest

The authors declare that they have no known competing financial interests or personal relationships that could have appeared to influence the work reported in this paper.

Acknowledgments

The study was supported by the Russian Science Foundation (Grant No. 21-72-00130). The specific heat measurements were supported by the subsidy allocated to Kazan Federal University for the state assignment in the sphere of scientific activities (Project No. 0671-2020-0050). The magnetic measurements, powder X-ray and EDX data were obtained using the analytical equipment of Krasnoyarsk Regional Center of Research Equipment of Federal Research Center "Krasnoyarsk Science Center SB RAS". The X-ray single-crystal experiment was done using the equipment of the Research and Education Centre "Molecular Design and Environmentally Safe Technologies" at NSU. The authors acknowledge Prof. Rushana Eremina and Dr. Tatyana Gavrilova for the valuable discussion of the obtained results.

Appendix A. Supplementary material

Supplementary data associated with this article can be found in the online version at doi:10.1016/j.jallcom.2022.163822.

References

[1] S.R. Bland, M. Angst, S. Adiga, V. Scagnoli, R.D. Johnson, J. Herrero-Martín, P.D. Hatton, Symmetry and charge order in Fe_2OBO_3 studied through polarized resonant x-ray diffraction, Phys. Rev. B 82 (2010) 115110.
[2] N.B. Ivanova, N.V. Kazak, Yu.V. Knyazev, D.A. Velikanov, A.D. Vasiliev, L.N. Bezmaternykh, M.S. Platunov, Structure and magnetism of copper-substituted cobalt ludwigite $Co_3O_2BO_3$, Low Temp. Phys. 39 (8) (2013) 709–713.
[3] Jitender Kumar, Soumendra Nath Panja, Deepak John Mukkattukavil, Arpan Bhattacharyya, A.K. Nigam, Sunil Nair, Reentrant superspin glass state and magnetization steps in the oxyborate Co_2AlBO_5, Phys. Rev. B 95 (2017) 144409.
[4] J. Schaefer, K. Bluhm, Zur Kristallstruktur von $Cu_2M(BO_3)O_2$ (M=Fe^{3+}, Ga^{3+}), Z. Anorg. Allg. Chem. 621 (1995) 571–575.
[5] F. Damay, J. Sottmann, F. Lainé, L. Chaix, M. Poienar, P. Beran, E. Elkaim, F. Fauth, L. Nataf, A. Guesdon, A. Maignan, C. Martin, Magnetic phase diagram for $Fe_{3-x}Mn_xBO_5$, Phys. Rev. B 101 (2020) 094418.
[6] M.A.V. Heringer, D.L. Mariano, D.C. Freitas, E. Baggio-Saitovitch, M.A. Continentino, D.R. Sanchez, Spin-glass behavior in $Co_3Mn_3(O_2BO_3)_2$ ludwigite with weak disorder, Phys. Rev. Mater. 4 (2020) 064412.
[7] E.M. Moshkina, T.P. Gavrilova, I.F. Gilmutdinov, A.G. Kiiamov, R.M. Eremina, Flux crystal growth of Cu_2GaBO_5 and Cu_2AlBO_5, J. Cryst. Growth 545 (2020) 125723.
[8] Evgeniya Moshkina, Clemens Ritter, Evgeniy Eremin, Svetlana Sofronova, Andrey Kartashev, Andrey Dubrovskiy, Leonard Bezmaternykh, Magnetic structure of Cu_2MnBO_5 ludwigite: thermodynamic, magnetic properties and neutron diffraction study, J. Phys. Condens. Matter 29 (2017) 245801.
[9] S. Sofronova, E. Moshkina, I. Nazarenko, Yu Seryotkin, S.A. Nepijko, V. Ksenofontov, K. Medjanik, A. Velizghanin, L. Bezmaternykh, Crystal growth, structure, magnetic properties and theoretical exchange interaction calculations of Cu_2MnBO_5, J. Magn. Magn. Mater. 420 (2016) 309–316.
[10] G.A. Petrakovskiĭ, L.N. Bezmaternykh, D.A. Velikanov, A.M. Vorotynov, O.A. Bayukov, M. Schneider, Magnetic properties of single crystals of ludwigites Cu_2MBO_5 (M = Fe^{3+}, Ga^{3+}), Phys. Solid State 51 (10) (2009) 2077–2083.
[11] Leonard Bezmaternykh, Evgeniya Moshkina, Evgeniy Eremin, Maxim Molokeev, Nikita Volkov, Yurii Seryotkin, Spin-lattice coupling and peculiarities of magnetic behavior of ferrimagnetic ludwigites $Mn^{2+}_{0.5}M^{2+}_{1.5}Mn^{3+}BO_5$ (M=Cu, Ni), Solid State Phenom. 233–234 (2015) 133–136.
[12] A.G. Gamzatov, Y.S. Koshkid'ko, D.C. Freitas, E. Moshkina, L. Bezmaternykh, A.M. Aliev, S.-C. Yu, M.H. Phan, Anisotropic magnetocaloric properties of the ludwigite single crystal Cu_2MnBO_5, Appl. Phys. Lett. 116 (2020) 232403.
[13] A.A. Dubrovsky, M.V. Rautskii, E.M. Moshkina, I.V. Yatsyk, R.M. Eremina, EPR-determined anisotropy of the g-factor and magnetostriction of a Cu_2MnBO_5 single crystal with a ludwigite structure, JETP Lett. 106 (2017) 716–719.
[14] Evgeniya Moshkina, Yurii Seryotkin, Asya Bovina, Maxim Molokeev, Evgeniy Eremin, Nadejda Belskaya, Leonard Bezmaternykh, Crystal formation of Cu-Mn-containing oxides and oxyborates in bismuth-boron fluxes diluted by MoO_3 and Na_2CO_3, J. Cryst. Growth 503 (2018) 1–8.
[15] R.M. Eremina, T.P. Gavrilova, E.M. Moshkina, I.F. Gilmutdinov, R.G. Batulin, V.V. Gurzhiy, V. Grinenko, D.S. Inosov, Structure, magnetic and thermodynamic properties of heterometallic ludwigites: Cu_2GaBO_5 and Cu_2AlBO_5, J. Magn. Magn. Mater. 515 (2020) 167262.
[16] A.A. Kulbakov, R. Sarkar, O. Janson, S. Dengre, T. Weinhold, E.M. Moshkina, P.Y. Portnichenko, H. Luetkens, F. Yokaichiya, A.S. Sukhanov, R.M. Eremina, Ph Schlender, A. Schneidewind, H.-H. Klauss, D.S. Inosov, Destruction of long-range magnetic order in an external magnetic field and the associated spin dynamics in Cu_2GaBO_5 and Cu_2AlBO_5 ludwigites, Phys. Rev. B103 (2021) 024447.
[17] E.M. Moshkina, M.S. Platunov, Yu.V. Seryotkin, A.F. Bovina, E.V. Eremin, S.N. Sofronova, L.N. Bezmaternykh, Transformation of structure and magnetic properties of Cu_2MnBO_5 under partial $Mn^{3+}\rightarrow Fe^{3+}$ substitution, J. Magn. Magn. Mater. 464 (2018) 1–10.
[18] Francoise Damay, Jonas Sottmann, Francois Fauth, Emmanuel Suard, Antoine Maignan, Christine Martin, High temperature spin-driven multiferroicity in ludwigite chromocuprate Cu_2CrBO_5, Appl. Phys. Lett. 118 (2021) 192903.
[19] P.M. Aiswarya, Rajesh Ganesan, R. Rajamadhavan, T. Gnanasekaran, Partial phase diagram of MoO_3 rich section of the ternary Bi-Mo-O system, J. Alloy. Compd. 745 (2018) 744–752.

[20] Rigaku Oxford Diffraction, CrysAlisPro Software system, Rigaku Corporation, Oxford, 2016.
[21] G. Sheldrick, SHELXT – integrated space-group and crystal-structure determination, Acta Crystallogr. A71 (2015) 3–8.
[22] D.A. Velikanov, High-sensitivity measurements of the magnetic properties of materials at cryogenic temperatures, Inorg. Mater. Appl. Res. 11 (4) (2020) 801–808.
[23] D.A. Velikanov, Magnetometer with a Superconducting Quantum Interferometric Sensor, RF Patent for the Invention RU 2481591 C1. Publ. 10.05. 2013, Bulletin No. 13.
[24] M.B. Irwin, R.C. Peterson, The crystal structure of ludwigite, Can. Mineral. 37 (1999) 939–943.
[25] Svetlana Sofronova, Rushana Eremina, Ivan Yatsyk, Evgeniya Moshkina, Exchange interactions in Cu_2AlBO_5 and Cu_2GaBO_5, AIP Conf. Proc. 2218 (2020) 040001.
[26] Sayandeep Ghosh, Deep Chandra Joshi, Prativa Pramanik, Suchit K. Jena, Suresh Pittala, Tapati Sarkar, Mohindar S. Seehra, Subhash Thota, Antiferromagnetism, spin-glass state, H–T phase diagram, and inverse magnetocaloric effect in Co_2RuO_4, J. Phys. Condens. Matter 32 (2020) 485806.
[27] Tapati Sarkar, V. Pralong, V. Caignaert, B. Raveau, Competition between ferrimagnetism and magnetic frustration in zinc substituted $YBaFe_4O_7$, Chem. Mater. 22 (2010) 2885–2891.
[28] C.A.M. Mulder, A.J. van Duynevelt, J.A. Mydosh, Susceptibility of the *Cu*Mn spin-glass: frequency and field dependencies, Phys. Rev. B 23 (3) (1981) 1384–1396.
[29] Cynthia P. Contreras Medrano, D.C. Freitas, D.R. Sanchez, C.B. Pinheiro, G.G. Eslava, L. Ghivelder, M.A. Continentino, Nonmagnetic ions enhance magnetic order in the ludwigite $Co_5Sn(O_2BO_3)_2$, Phys. Rev. B 91 (2015) 054402.
[30] D.V. Popov, T.P. Gavrilova, I.F. Gilmutdinov, M.A. Cherosov, V.A. Shustov, E.M. Moshkina, L.N. Bezmaternykh, R.M. Eremina, Magnetic properties of ludwigite $Mn_{2.25}Co_{0.75}BO_5$, J. Phys. Chem. Solids 148 (2021) 10969.
[31] S. Chikazumi, Physics of Ferromagnetism, Oxford University Press, New York, 1997, pp. 15–17.
[32] E.E. Bragg, M.S. Seehra, Magnetic susceptibility of MnF, near T and Fisher's relation, Phys. Rev. B 7 (9) (1973) 4197–4202.
[33] V. Narang, D. Korakakis, M.S. Seehra, Nature of magnetism and magnetic-field-induced transitions in non-collinear antiferromagnet Er_2O_3, J. Magn. Magn. Mater. 368 (2014) 353.
[34] P. Dutta, M.S. Seehra, S. Thota, J. Kumar, A comparative study of the magnetic properties of bulk and nanocrystalline Co_3O_4, J. Phys. Condens. Matter 20 (2007) 015218.
[35] Evgeniya Moshkina, Svetlana Sofronova, Alexey Veligzhanin, Maxim Molokeev, Ilya Nazarenko, Evgeniy Eremin, Leonard Bezmaternykh, Magnetism and structure of Ni_2MnBO_5 ludwigite, J. Magn. Magn. Mater. 402 (2016) 69–75.
[36] G.A. Bain, J.F. Berry, Diamagnetic corrections and Pascal's constants, J. Chem. Educ. 85 (4) (2008) 532–536.
[37] J.A. Souza, J.J. Neumeier, R.K. Bollinger, B. McGuire, C.A.M. dos Santos, H. Terashita, Magnetic susceptibility and electrical resistivity of $LaMnO_3$, $CaMnO_3$, and $La_{1-x}Sr_xMnO_3$ ($0.13 \leq x \leq 0.45$) in the temperature range 300–900 K, Phys. Rev. B 76 (2007) 024407.
[38] M.G. Banks, R.K. Kremer, C. Hoch, A. Simon, B. Ouladdiaf, J.-M. Broto, H. Rakoto, C. Lee, M.-H. Whangbo, Magnetic ordering in the frustrated Heisenberg chain system cupric chloride $CuCl_2$, Phys. Rev. B 80 (2009) 024404.
[39] M.E. Lines, Camparative studies of Magnetism in $KNiF_3$ and K_2NiF_4, Phys. Rev. 164 (2) (1967) 736–748.
[40] L. Cornu, M. Duttine, M. Gaudon, V. Jubera, Luminescence switch of Mn-Doped $ZnAl_2O_4$ powder with temperature, J. Mater. Chem. C 2 (2014) 9512–9522.
[41] B.V. Padlyak, W. Wojtowicz, V.T. Adamiv, Ya.V. Burak, I.M. Teslyuk, EPR spectroscopy of the Mn^{2+} and Cu^{2+} centres in lithiumand potassium–lithium tetraborate glasses, Acta Phys. Pol. 117 (1) (2010) 122–125.
[42] (a) R.M. Eremina, T.P. Gavrilova, N.A. Krug von Nidda, et al., Anisotropic exchange interactions in $CuTe_2O_5$, Phys. Solid State 50 (2008) 283–289;
(b) R.M. Krishna, S.K. Gupta, Electron paramagnetic resonance investigations of the Cu^{2+} ion in a variety of host lattices – a review, Bull. Magn. Res. 16 (1994) 239–291.